Supplement of Atmos. Chem. Phys., 16, 1303–1315, 2016
http://www.atmos-chem-phys.net/16/1303/2016/
doi:10.5194/acp-16-1303-2016-supplement

Atmospheric Chemistry and Physics Open Access EGU

Supplement of

Observed high-altitude warming and snow cover retreat over Tibet and the Himalayas enhanced by black carbon aerosols

Y. Xu et al.

Correspondence to: Y. Xu (yangyang@ucar.edu)

Supplementary materials

Supplementary references

Lawrence, D. M., Oleson, K. W., Flanner, M. G., Thornton, P. E., Swenson, S. C., Lawrence, P. J., Zeng, X., Yang, Z.-L., Levis, S., Sakaguchi, K., Bonan, G. B., and Slater, A. G.: Parameterization improvements and functional and structural advances in Version 4 of the Community Land Model, J. Adv. Model. Earth Syst., 3, 1–27, doi:10.1029/2011MS000045, 2011.

Ménégoz, M., Gallée, H., and Jacobi, H. W.: Precipitation and snow cover in the Himalaya: from reanalysis to regional climate simulations, Hydrol. Earth Syst. Sci., 17, 3921–3936, doi:10.5194/hess-17-3921-2013, 2013.

Robinson, D. A., Estilow, T. W., and NOAA CDR Program: NOAA Climate Date Record (CDR) of Northern Hemisphere (NH) Snow Cover Extent (SCE), Version 1, NOAA National Climatic Data Center, doi:10.7289/V5N014G9, 2012.

Willmott, C. J. and Matsuura, K.: Terrestrial Air Temperature and Precipitation: Monthly and Annual Time Series (1950–1999), http://climate.geog.udel.edu/~climate/html_pages/README.ghcn_ts2.html, 2001.

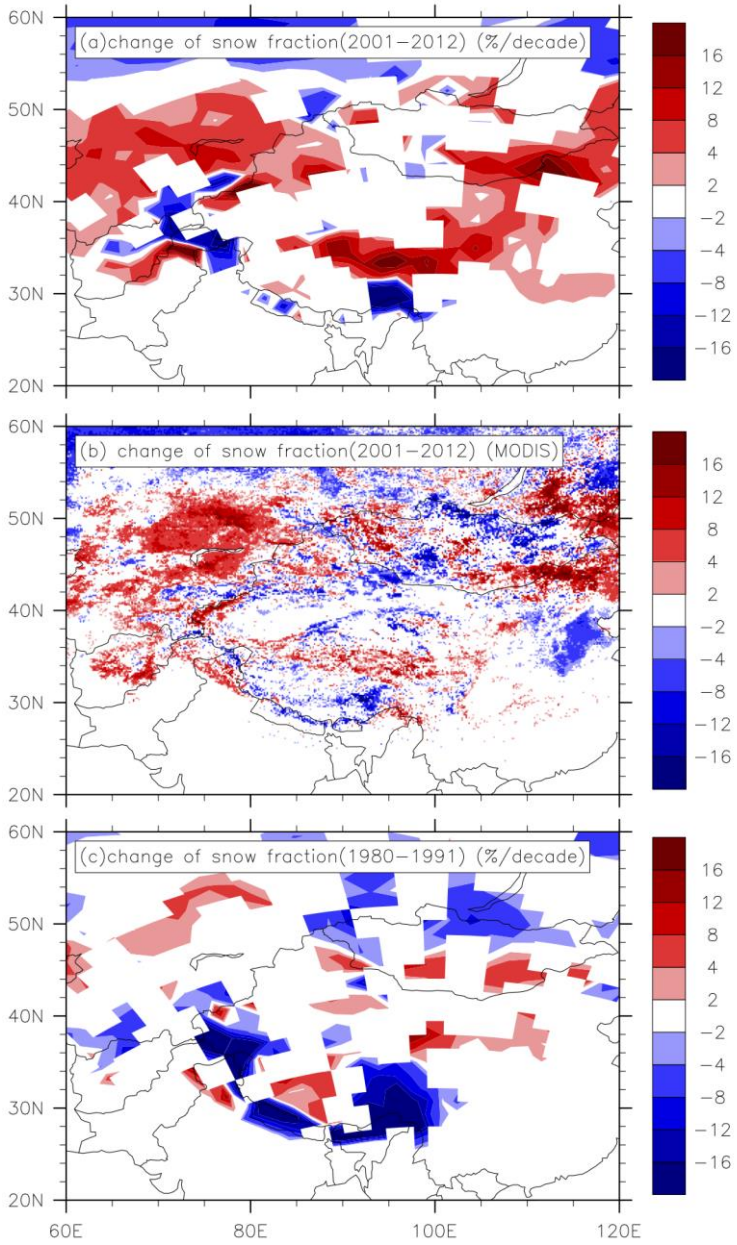

Fig. S1. (a) Snow cover extent same as Fig. 1, but for 2001-2012. (b) same as (a) but from MODIS. (c) same as (a) but for 1980-1991.

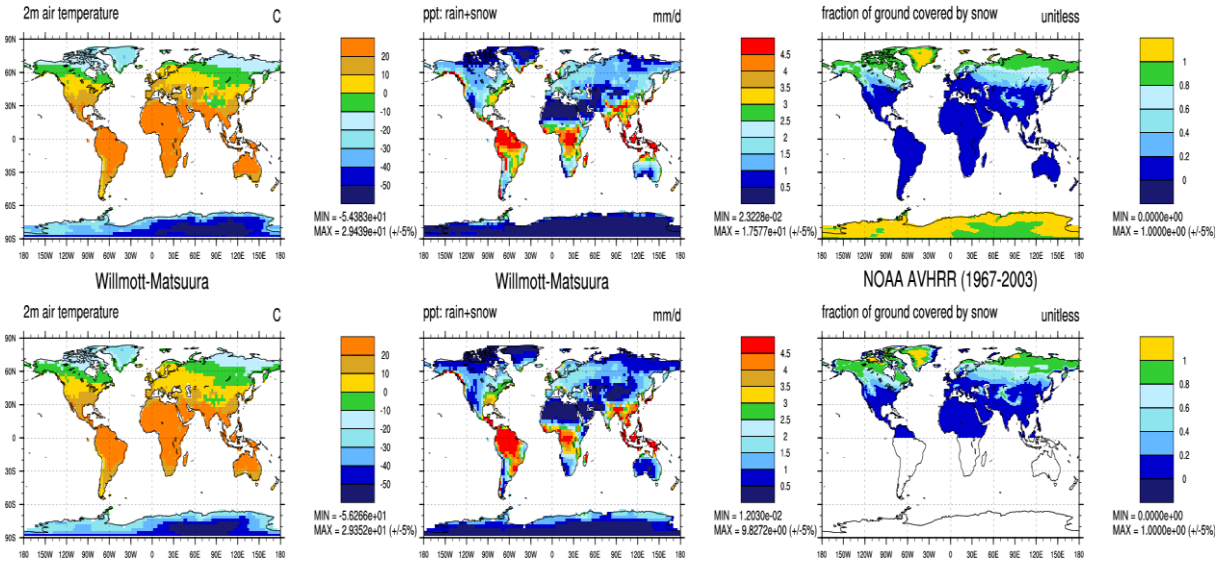

Fig. S2. (Left) climatological surface air temperature (ºC) in the model simulation in the top panel, and observed surface air temperature in the bottom panel. (Middle) total precipitation (rain and snow fall) (mm/day) (Right) snow cover fraction. The model results in the top row are the 1981-2005 averages of the transient simulations under all radiative forcing. The temperature and precipitation observations are from updated dataset of Willmott and Matsuura (2001). The snow cover observations are from NOAA AVHRR as compiled by Robinson et al., (2012). In terrain-complex regions (such as North American Rockies, South American Andes and Tibet Plateau), the model tends to overestimate the precipitation and consequently snow cover, a bias commonly found in global climate model with coarse resolutions (Ménégoz et al., 2013). More detailed land model evaluations can be found in Lawrence et al., (2011).

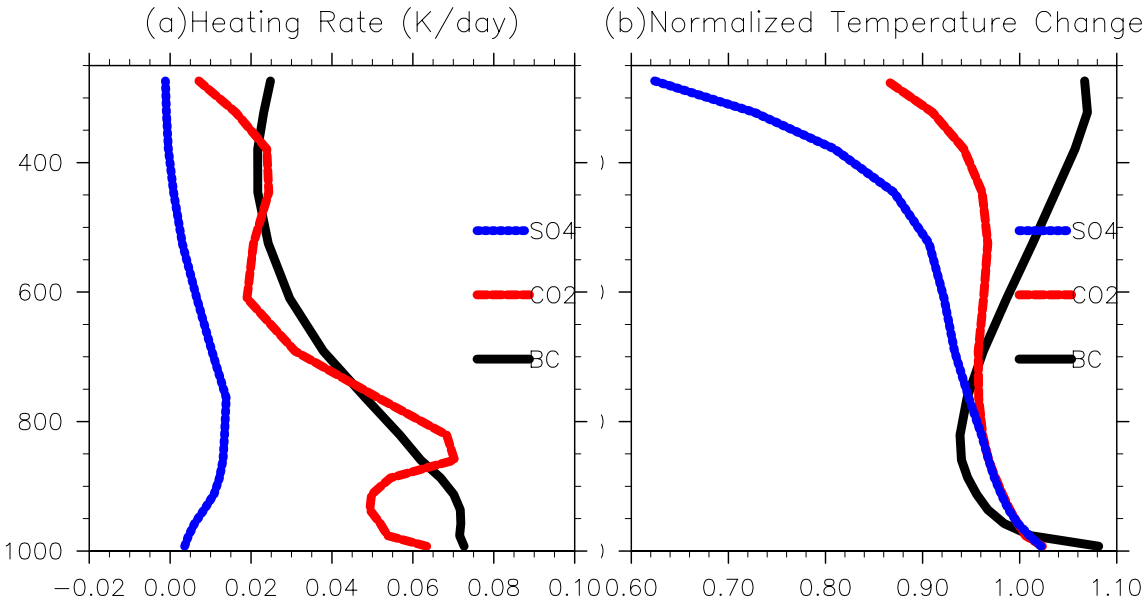

Fig. S3. Similar to Fig. 3 but showing the vertical profile averaged over the Tibet region. (a) Radiative heating rate (ºC/day). Shortwave fluxes for BC and SO_4, and longwave flux for CO_2. (b) Normalized temperature change relative to the average below 900 hPa. Note that the changes are tropospheric atmospheric temperature change, not surface temperature. The domains of the Tibet Plateau (as in Table 1) are 30 to 40ºN and 80 to 100ºE.

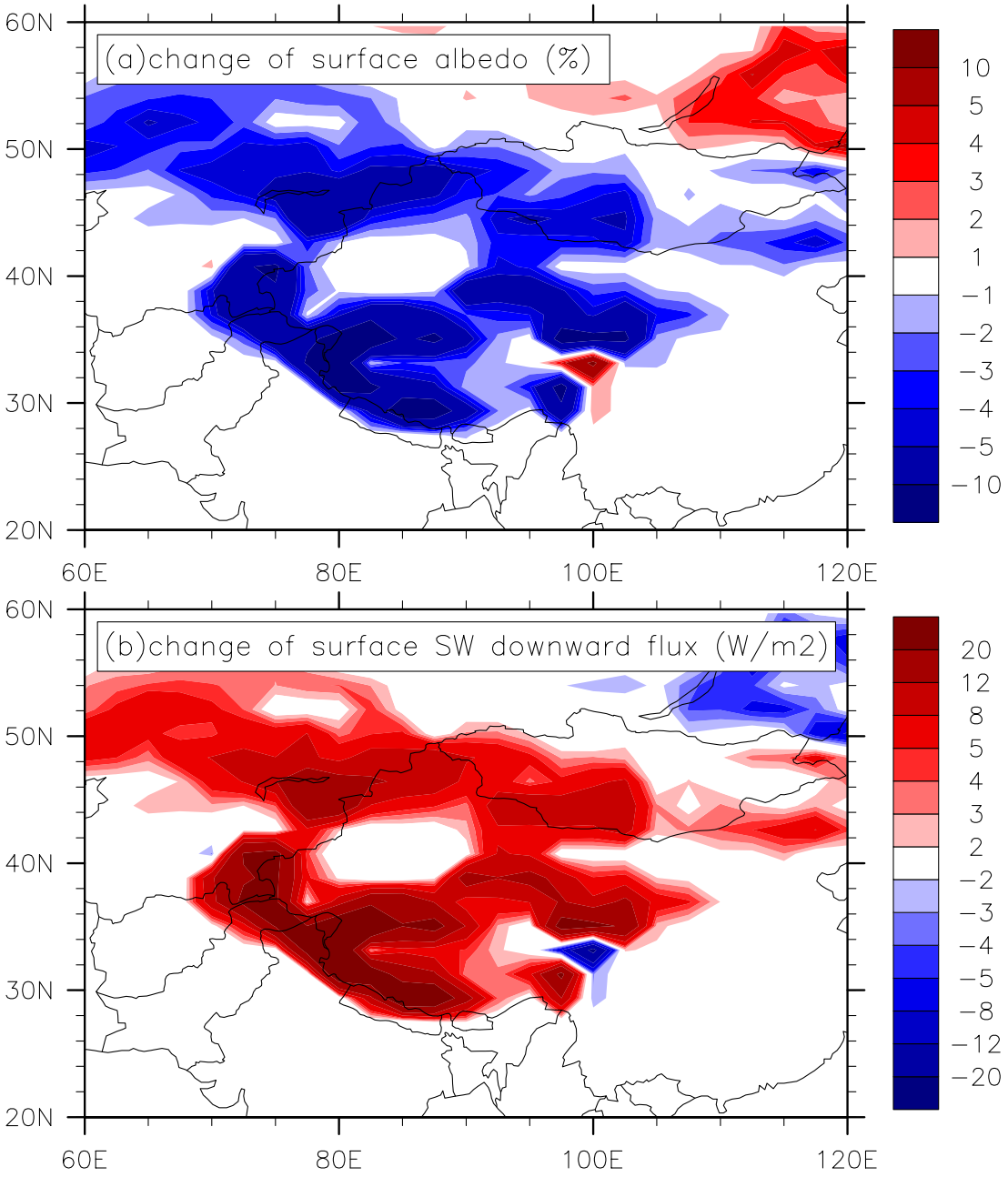

Fig. S4. (a) Change of surface albedo due to BC deposition on snow; (b) Change of net shortwave radiation (downward as positive, W/m^2). Over Tibet Plateau, the surface albedo is reduced by 2.2%, causing an increase in shortwave radiation reaching the surface by 4.1 W/m^2 (heating). Globally, the radiative forcing at the surface is about 0.1 W/m^2. The change of surface albedo in (a) is calculated with the five-year atmosphere-only simulation in which BC emission is increased. Therefore, the albedo change largely represents the surface darkening effects due to BC deposition, although we cannot completely rule out the associated melting during this period. As a result, the actual radiative forcing at the surface due to BC in snow should be smaller than that in (b).